Dual Source Fourier Transform Polarization Modulation Spectroscopy: An Improved Method for the Measurement of Circular and Linear Dichroism

LAURENCE A. NAFIE,* HENRY BUIJS, ALLAN RILLING, XIAOLIN CAO, and RINA K. DUKOR

Department of Chemistry, Syracuse University, Syracuse, New York 13244-4100 (L.A.N., X.C.); ABB Bomem, 585, Charest Blvd. East, Quebec (Quebec) G1K 9H4, Canada (H.B., A.R.); and BioTools, Inc., 950 N. Rand Road, Unit 123, Wauconda, Illinois 60084 (R.K.D., L.A.N.)

It is shown that the use of two sources in a four-port interferometer equipped with cube-corner mirrors leads to increased signal-to-noise ratios in Fourier transform (FT-IR) circular and linear dichroism spectra. The output beam to the sample is a superposition of two interferograms, one from each source, having opposite Fourier phases. These two interferograms cancel one another to the degree that the two sources are matched in intensity. If the radiation from each of the two sources is first polarized orthogonally with respect to the other and passed through a polarization modulator before reaching the sample, the resulting polarization-modulation interferograms are out of Fourier phase and out of polarization-modulation phase. As a result, the polarization-modulation interferograms, due to circular or linear dichroism in the sample, from the two sources combine positively rather than negatively. An improvement in signal-to-noise ratio of up to two (or a factor of four in scan-time reduction for the same signal-to-noise ratio) compared to single source operation can be realized, while at the same time, the potential for saturation of the detector signal is significantly reduced due to the reduction in magnitude of the combined ordinary infrared transmission interferogram. Absorption and circular dichroism spectra from a dual-source FT-IR spectrometer are presented and analyzed.

Index Headings: **Fourier transform infrared; Polarization modulation; Vibrational circular dichroism; Vibrational linear dichroism; Signal-to-noise ratio optimization.**

INTRODUCTION

The measurement of small spectral intensities associated with polarization differences in samples is often limited in quality by the lower than desired signal-to-noise ratios. This is particularly true for Fourier transform infrared (FT-IR) vibrational circular dichroism (VCD), the difference in absorbance of a molecule for left versus right circularly polarized radiation, where intensities are commonly in the range 10^{-4} to 10^{-6} absorbance units.[1–7] An obvious way to improve signal quality is to increase the instrumental throughput for a given spectral region of measurement. However, this is often limited by the onset of detector nonlinearity at high infrared intensity levels, thus effectively limiting the further improvement in intrinsic signal-to-noise ratio of the FT-VCD measurement.

In order to carry out VCD measurements with an FT-IR spectrometer, the so-called double modulation method was developed over twenty years ago.[7–10] Using this method for VCD measurement, the infrared beam is first polarized linearly at 45 degrees to the stress axis of a photoelastic modulator (PEM) that converts the polarization state of the light to left and right circular states at the PEM frequency, typically in the tens of kHz frequency range. The beam then passes through a chiral sample and onto a semiconductor detector that can follow the high-frequency polarization modulation signal. The signal at the detector has two kinds of intensity modulation, one at the Fourier frequencies associated with the unpolarized IR spectrum and one at the PEM modulation frequency associated with the VCD spectrum. To measure VCD, the signal is first demodulated at the PEM frequency and the resulting VCD interferogram is Fourier transformed to yield the VCD spectrum. If the linear polarizer prior to the PEM is rotated by 90 degrees, right (RCP) and left circular polarization (LCP) states of radiation are interchanged and the resulting VCD spectrum has the opposite sign for all of its bands. The double modulation method can also be applied to the measurement of vibrational linear dichroism (VLD) in an analogous way, using instead modulation of the IR beam between vertically and horizontally polarized radiation, and the rotation of the linear polarizer by 90 degrees changes the sign of the VLD spectrum as well.[11–13]

Most interferometers have two ports, an input port for radiation from the source, and an output port for the beam going to the sample.[14,15] A four-port interferometer can be constructed if the plane mirrors of a conventional interferometer are replaced by cube-corner mirrors. In such an interferometer, the incident beam from the source is directed to the lower half of the beamsplitter. There, in the usual fashion, the source beam is divided into a transmitted beam, I_T, and a reflected beam, I_R, and directed to the lower half of the two cube-corner mirrors of the interferometer. Each optical ray undergoes three reflections, one off each of the three surfaces of the cube-corner mirror, and returns along a path exactly parallel to its incident path to the upper half of the beamsplitter. Here the two beams recombine and interfere to create two output beams from the interferometer, I_{TR+RT} and I_{TT+RR}. One of these beams, typically, I_{TR+RT}, travels to the sample region and the other, I_{TT+RR}, travels back toward the source. These beams are illustrated for a one-source interferometer in the upper part of Fig. 1. In a conventional interferometer, only the sample beam is available, whereas in the cube-corner interferometer where the source beam is confined to the lower half of the interferometer, both beams are available on the upper half of the optical lay-

Received 14 November 2003; accepted 28 January 2004.
* Author to whom correspondence should be sent.

0003-7028/04/5806-0647$2.00/0

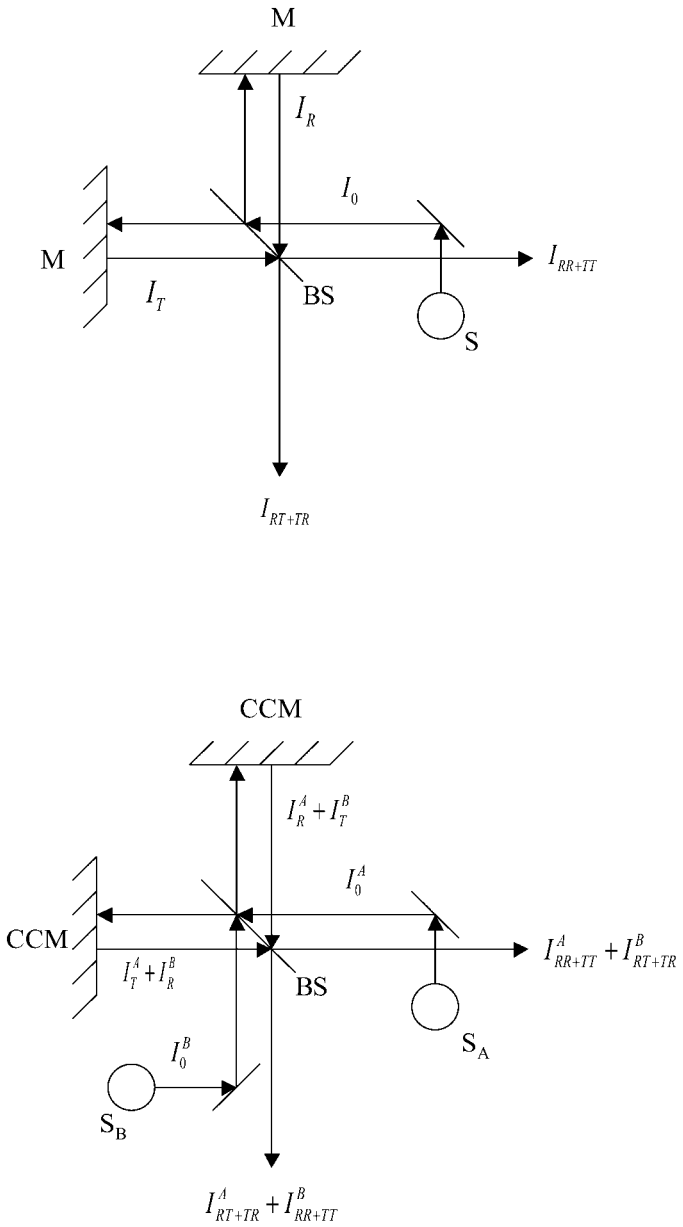

FIG. 1. Diagram illustrating the optical layout of (**upper**) single-source and (**lower**) dual-source interferometers. The two sources in the dual source case are labeled S_A and S_B, and the ZnSe beamsplitter is labeled BS. The reflections occur at cube-corner mirrors (CCM) that displace the outgoing parallel beam relative to the incoming beam but do not change the final linear polarization state.

out. With this design, it is possible to construct an interferometer with two sources with inputs on the lower level of the interferometer and two output beams on the upper level. The interferometer is symmetric with respect to the directions of the input and output beams. Typically either one source or the other is used, but it is noted that the output beams of the two sources are out of Fourier phase with respect to one another along a given output beam path. If both sources are operated at the same time, their interferograms tend to cancel to the degree that the two sources have the same output modulation intensity and spectral profile. The beams used in a two-source four-port interferometer are illustrated in the lower half of Fig. 1.

In this paper, we describe a method to combine a four-port dual-source interferometer with double modulation FT-VCD or FT-VLD measurements to obtain a spectrometer with enhanced signal quality and lower susceptibility to detector saturation. The method involves placing a linear polarizer in front of each of the two sources in the interferometer and setting the polarization state of one to be vertical and the other to be horizontal. In this way, the ordinary infrared interferograms from the two sources combine negatively since they are simply out of Fourier phase with respect to one another. However, the polarization-modulation interferograms combine positively since they are both out of Fourier phase and out of polarization-modulation phase with respect to each other. The polarization phase inversion created by orthogonal linear polarizers in front of the two sources undoes the Fourier phase reversal so the VCD or VLD interferograms become larger at the same time that the ordinary infrared-transmission interferograms become smaller.

THEORETICAL BACKGROUND

Single-Source Infrared. We first consider an interferometer equipped with a single source. An optical diagram is given in the upper half of Fig. 1 that shows the beams produced by the source and interferometer, one going to the sample position, I_{RT+TR}, and the other returning to the source, I_{RR+TT}. The beam traveling to the sample experiences either reflection (R) followed by transmission (T), or the reverse, at the beamsplitter, while the beam traveling back toward the source experiences either two reflections or two transmissions at the beamsplitter. The standard theoretical expressions for these two beams are given by:

$$I_{RT+TR}(\delta) = 2a_T a_R I_0 - 2a_T a_R \int_0^\infty I_0(\bar{\nu}) e^{2\pi i \delta \bar{\nu}} \, d\bar{\nu} \qquad (1)$$

$$I_{RR+TT}(\delta) = (a_R^2 + a_T^2) I_0 + 2a_T a_R \int_0^\infty I_0(\bar{\nu}) e^{2\pi i \delta \bar{\nu}} \, d\bar{\nu} \qquad (2)$$

where δ is the interferometer beam-path difference. In general, the beamsplitter coefficients, a_R for reflection, and a_T for transmission efficiency, are different. Each beam has a constant DC intensity contribution (first term) and a Fourier-modulated AC intensity (second term), and the Fourier terms of the two beams are out of phase with respect to each other and are given opposite signs. For simplicity, we have assumed a constant value of the efficiency coefficients over the spectral range of interest, and the sum of a_R and a_T is equal to unity:

$$a_R + a_T = 1 \qquad (3)$$

Given this constraint, it is clear that the sum of the two output beams equals the original source intensity, I_0. The effects of internal reflections within the beamsplitter are included in the transmission and reflection efficiency coefficients. At the equal mirror position, $\delta = 0$, the Fourier integrals in Eqs. 1 and 2 reduce to the integral of the intensity of the source as:

$$I_0 = \int_0^\infty I_0(\bar{\nu}) \, d\bar{\nu} \qquad (4)$$

and, as observed experimentally, all intensity returns to the source in the beam I_{RR+TT} and none appears at the sample in the beam I_{RT+TR}. For unequal values of the transmission and reflection coefficients, the DC component of I_{RR+TT} is always greater than that of I_{RT+TR} (alternatively designated the 2*RT* beam). On the other hand, the Fourier modulated components of each of these intensities that arises from interference between the beams returning from the two arms of the interferometer must be equal, and the amount of the radiation in the 2*RT* beam limits this Fourier-modulated intensity. The highest Fourier modulation efficiency occurs when a_R and a_T are equal to one another with a value of ½.

Dual-Source Infrared. In a four-port interferometer equipped with two input sources and cube-corner mirrors, as described above, there are four output beams to consider, two from source *A* and two from source *B*. For simplicity, the case of equal reflection and transmission efficiency coefficients is considered first. The output beams passing by source *B* and by source *A* in Fig. 1 are given by Eqs. 5 and 6, respectively:

$$I^A_{RT+TR}(\delta) + I^B_{RR+TT}(\delta) = \frac{1}{2}(I^A_0 + I^B_0) - \frac{1}{2}\int_0^\infty [I^A_0(\bar{\nu}) - I^B_0(\bar{\nu})]e^{2\pi i\delta\bar{\nu}}\,d\bar{\nu} \quad (5)$$

$$I^A_{RR+TT}(\delta) + I^B_{RT+TR}(\delta) = \frac{1}{2}(I^A_0 + I^B_0) + \frac{1}{2}\int_0^\infty [I^A_0(\bar{\nu}) - I^B_0(\bar{\nu})]e^{2\pi i\delta\bar{\nu}}\,d\bar{\nu} \quad (6)$$

Here again, the two output beams are out of Fourier phase with respect to each other and the sum of these two equations is the sum of the two total source intensities. In addition, the contributions of sources *A* and *B* in each of these two beams are also out of Fourier phase with respect to each other. If the two sources have the same total intensity and the same spectral profiles, namely, $I^A_0(\bar{\nu}) = I^B_0(\bar{\nu})$, the Fourier integrals in Eqs. 5 and 6 vanish.

Next we consider the case of the four-port cube-corner-mirror interferometer with two sources where polarizers are placed in front of each source aligned with their polarization axes orthogonal to each other. In particular, we consider the case where the polarization of source *A* is vertical with respect to the plane of the arms of the interferometer and radiation from source *B* is horizontally polarized. For source *A*, the efficiency coefficients for reflection and transmission at the beamsplitter are those for *s*-polarized radiation with respect to the surface of the beamsplitter. Similarly, for source *B*, the efficiency coefficients are those for *p*-polarized radiation. In general, efficiency coefficients for *s*- and *p*-polarized radiation for reflection and transmission are not equal to one another. Generalizing Eqs. 5 and 6 to contain these four coefficients, we have:

$$I^A_{RT+TR}(\delta) + I^B_{RR+TT}(\delta) = 2a^s_R a^s_T I^A_0 + [(a^p_R)^2 + (a^p_T)^2]I^B_0 - \int_0^\infty [2a^s_R a^s_T I^A_0(\bar{\nu}) - 2a^p_R a^p_T I^B_0(\bar{\nu})]e^{2\pi i\delta\bar{\nu}}\,d\bar{\nu} \quad (7)$$

$$I^A_{RR+TT}(\delta) + I^B_{RT+TR}(\delta) = 2a^p_R a^p_T I^B_0 + [(a^s_R)^2 + (a^s_T)^2]I^A_0 + \int_0^\infty [2a^s_R a^s_T I^A_0(\bar{\nu}) - 2a^p_R a^p_R I^B_0(\bar{\nu})]e^{2\pi i\delta\bar{\nu}}\,d\bar{\nu} \quad (8)$$

Here again the sums of the transmission and reflection coefficients for *s*- and *p*-polarized radiation are both unity, namely:

$$a^s_R + a^s_T = a^p_R + a^p_T = 1 \quad (9)$$

For these expressions the sum of the two equations is simply the integrated sum of the two sources. The interferograms are equal and opposite and the contributions of each source to the interferograms of each beam are opposite. If all four efficiency coefficients in Eq. 9 are equal to ½, Eqs. 7 and 8 reduce to Eqs. 5 and 6. In general, for Eqs. 7 and 8 there are two ways in which the ordinary infrared-intensity interferograms can avoid vanishing. One is if the source intensities and profiles are different, and the other is if the corresponding efficiency coefficients of the beamsplitter for *s*- and *p*-polarized radiation are not the same. In general, the products $a^s_R a^s_T$ and $a^p_R a^p_T$ are not equal. Therefore, even if the two sources are matched to be equal, the transmission interferograms in Eqs. 7 and 8 will not vanish.

Single-Source Vibrational Circular Dichroism. In the case of FT-VCD measurements using the double modulation method, a PEM is placed in the beam after a linear polarizer and before the sample. If the sample is chiral, there will be differences in the transmitted light at the PEM modulation frequency due to differences in the absorbance of the sample for left versus right circularly polarized radiation. Thus, at the detector, there will be DC terms and Fourier-modulated terms, as discussed above, as well as terms that are double-modulated at the Fourier frequencies and the PEM frequency. The interferogram associated with the VCD is obtained by demodulating the double-modulated term with respect to the PEM frequency using a lock-in amplifier tuned to this frequency. The output of the lock-in with a sufficiently fast time constant, typically in the microsecond range, yields the VCD interferogram. If VCD detection and a chiral sample are added to the setup described by Eq. 1, the total intensity expression, after demodulation of the polarization-modulation interferogram at the PEM frequency, is:

$$I_{TR+RT}(\delta) = 2a_T a_R I_0 - 2a_T a_R \int_0^\infty I(\bar{\nu})e^{2\pi i\delta\bar{\nu}}\,d\bar{\nu} - 2a_T a_R \int_0^\infty I(\bar{\nu})2J_1[\alpha(\bar{\nu})]1.1513\Delta A(\bar{\nu})e^{2\pi i\delta\bar{\nu}}\,d\bar{\nu} \quad (10)$$

The absorbance $A(\bar{\nu})$ of the sample is defined by the expression:

$$A(\bar{\nu}) = -\log_{10}[I(\bar{\nu})/I_0(\bar{\nu})] \quad (11)$$

and VCD is defined as:

$$\Delta A(\bar{\nu}) = A_L(\bar{\nu}) - A_R(\bar{\nu}) \quad (12)$$

In Eq. 10, $J_1[\alpha(\bar{\nu})]$ is the PEM efficiency with respect to VCD measurement as a function of wavenumber frequency. The wavenumber frequency of the maximum of $J_1[\alpha(\bar{\nu})]$ can be set by adjusting the level of the PEM voltage. The first two terms in Eq. 10 are the same as those in Eq. 1 for the IR interferogram. The third term in Eq. 10 is the VCD interferogram. The VCD spectrum can be isolated in a three-step process by separately Fourier transforming the second and third terms in Eq. 10, dividing the FT of the third term by the FT of the second term, and finally removing the Bessel function dependence by dividing by an appropriate calibration curve, $2J_1[\alpha(\bar{\nu})]1.1513$, the procedure for the measurement of which has been published previously.[9,13] This procedure is expressed as:

$$\Delta A(\bar{\nu}) = \frac{FT\left\{2a_T a_R \int_0^\infty I(\bar{\nu}) 2J_1[\alpha(\bar{\nu})]1.1513 \Delta A(\bar{\nu}) e^{2\pi i \delta \bar{\nu}}\, d\bar{\nu}\right\}}{FT\left[2a_T a_R \int_0^\infty I(\bar{\nu}) e^{2\pi i \delta \bar{\nu}}\, d\bar{\nu}\right] 2J_1[\alpha(\bar{\nu})]1.1513} \quad (13)$$

Dual-Source Vibrational Circular Dichroism. We can generalize the VCD interferogram term in Eq. 10 for the case of dual source with vertical and horizontal polarizers, given in Eqs. 7 and 8, as:

$$[I^A_{RT+TR}(\delta) + I^B_{RR+TT}(\delta)]_{VCD} = -\int_0^\infty [2a^s_R a^s_T I^A(\bar{\nu}) + 2a^p_R a^p_T I^B(\bar{\nu})] \times 2J_1[\alpha(\bar{\nu})]\Delta A(\bar{\nu}) e^{2\pi i \delta \bar{\nu}}\, d\bar{\nu} \quad (14)$$

$$[I^A_{RR+TT}(\delta) + I^B_{RT+TR}(\delta)]_{VCD} = \int_0^\infty [2a^s_R a^s_T I^A(\bar{\nu}) + 2a^p_R a^p_T I^B(\bar{\nu})] \times 2J_1[\alpha(\bar{\nu})]\Delta A(\bar{\nu}) e^{2\pi i \delta \bar{\nu}}\, d\bar{\nu} \quad (15)$$

The two terms that depend on the beamsplitter efficiency coefficients and the infrared intensities due to the two sources now combine by addition, rather than by subtraction as in Eqs. 7 and 8. This is because the VCD contributions from the two sources have the opposite signs due to the orthogonal orientations of their polarizers, whereas the relative orientation of the polarizers has no such effect for the ordinary infrared intensity or absorbance spectrum. Since, as we demonstrated above, the two sources carry intrinsically opposite Fourier phase for their contributions to a given output beam, the VCD contributions from each source add rather than subtract. It is interesting to note that the VCD interferograms associated with the two output beams, namely those in Eqs. 14 and 15, are identical in magnitude but opposite in sign.

Finally, we can compare the expected magnitude of the VCD intensity from dual-source operation, $[\Delta A(\bar{\nu})]_{DS}$, to that of single source operation, $[\Delta A(\bar{\nu})]_{SS}$, where the latter is given by Eq. 13. Since the VCD intensity involves dividing the VCD transmission spectrum by the corresponding infrared transmission spectrum, as illustrated in Eq. 13, we can write:

$$[\Delta A(\bar{\nu})]_{DS} = \frac{a^p_R a^p_T I^A(\bar{\nu}) + a^s_R a^s_T I^B(\bar{\nu})}{|a^p_R a^p_T I^A(\bar{\nu}) - a^s_R a^s_T I^B(\bar{\nu})|}[\Delta A(\bar{\nu})]_{SS} \quad (16)$$

This ratio is the sum of two positive terms divided by the positive difference of those same two terms. It is independent of wavenumber frequency, assuming wavenumber-independent efficient coefficients, and is the same for each of the two output beams from the four-port, dual-source interferometer. Because the efficiency coefficients are defined as positive numbers, the ratio is always greater than unity for unequal contributions from sources *A* and *B*. The ratio reduces to unity if either source is turned off, the sign of the denominator, before taking the absolute value, being immaterial physically as it is always positive following Fourier transformation with appropriate phase correction. There is no limit to the increase in the magnitude of the measured dual-source uncalibrated VCD intensity relative to single-source uncalibrated VCD intensity as the denominator in Eq. 16 approaches zero.

Another numerical measure of dual-source to single-source operation efficiency is to compare the magnitude of the dual-source infrared transmission intensity to either of the two single-source infrared transmission intensities, such as for comparison to source *A*:

$$\frac{I^A_{TR+RT}(\bar{\nu}) + I^B_{RR+TT}(\bar{\nu})}{I^A_{TR+RT}(\bar{\nu})} = \frac{|a^s_R a^s_T I^A(\bar{\nu}) - a^p_R a^p_T I^B(\bar{\nu})|}{a^s_R a^s_T I^A(\bar{\nu})} \quad (17)$$

and analogously for comparison to source *B*. Measurement of the magnitudes of the two single-source intensity interferograms allows prediction of the magnitude of the dual-source interferogram.

Analogous expressions can be written for linear dichroism, rather than circular dichroism measurements. In the case of VLD, a linearly dichroic sample is measured. Such a sample has a difference in absorption intensity for orthogonally polarized linear polarization states. Hence, the sample requires some degree of macroscopic orientation and must possess one or more internal axes of alignment. Examples are a stretched polymer film or fiber, or grazing-angle incidence and reflection off a surface with adsorbed molecules, the latter case often being referred to as infrared reflection absorption spectroscopy (IRRAS).[12] Dual-source operation is analogous for VCD and VLD because changing the orientation of the polarizer by 90° prior to the PEM changes the sign of the entire VLD spectrum. The only changes in these expressions are the usual ones when comparing expressions for VCD and VLD, namely the VLD spectrum depends on $J_2[\alpha(\bar{\nu})]$ instead of $J_1[\alpha(\bar{\nu})]$ and the VLD interferogram is present at the harmonic of (twice) the PEM frequency instead of the fundamental of the PEM frequency.

EXPERIMENTAL

Fourier transform vibrational circular dichroism measurements were carried out on the Chiral*IR* from Bio-Tools, Wauconda, IL, and ABB-Bomem, Quebec, Canada, equipped for dual-source operation with a four-port cube-corner mirror interferometer and a ZnSe photoelastic modulator (PEM) operating at 37 kHz. Infrared radiation was detected with a liquid-nitrogen-cooled MCT detector having a low-frequency cut-off of approximately

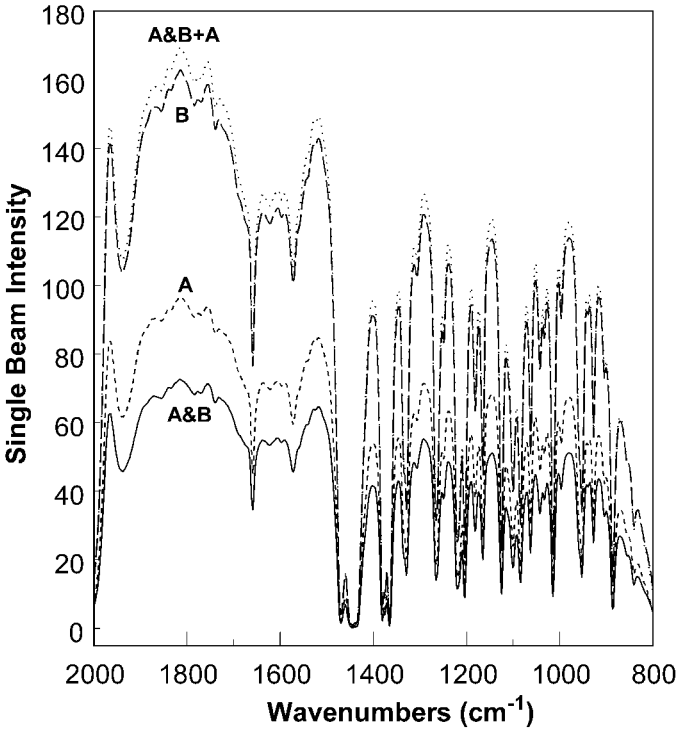

FIG. 2. Single-source (**A** and **B**) and dual-source (**A&B**) single-beam infrared transmission spectra of *S*-(−)-α-pinene, neat in a 69 μm cell at 4 cm^{-1} resolution. The calculated curve labeled **A&B+A** can be compared to single-source curve **B**.

800 cm^{-1}. The beamsplitter is constructed from uncoated ZnSe. The interferometer is equipped with two sources, *A* and *B*. Source *A* is in the normal source position and has a BaF_2 wire grid polarizer placed in front of it to pass vertically polarized radiation with respect to the plane of the interferometer. For reflection or transmission with respect to the plane of the beamsplitter, the radiation from this source is *s*-polarized. Source *B* is located beneath the beam port that normally goes to the sample. The radiation is horizontally polarized and corresponds to *p*-polarized radiation at the beamsplitter. VCD and IR spectra of *S*-(−)-α-pinene were measured at 4 cm^{-1} resolution employing standard VCD spectral collection and calibration software on the Chiral*IR* spectrometer. Samples of *S*-(−)-α-pinene were purchased from the Aldrich Chemical Company and used without further purification.

RESULTS

In Fig. 2, we present the results of single-beam IR transmission measurements in arbitrary units for a sample of *S*-(−)-α-pinene showing the relative intensities for source *A* (labeled A), source *B* (B), and both sources *A* and *B* (A&B). It is clear that reduced single-beam transmission is obtained in the case of two sources corresponding to the difference in the single-beam transmission spectra for source *A* and source *B*. In addition, we provide a combined curve labeled A&B+A that can be compared directly to curve B since source *A* contributes negatively to the A&B intensity and since (B − A) + A equals B. Under our normal operating conditions, the single-beam transmission for source *B* for the spectral region between 2000 to 800 cm^{-1} saturates the detector. With a sample of α-pinene in place, source *B* does not saturate the detector; however, the transmission level is not far from saturation. The small difference in the transmission for curves A&B+A and B arises from the onset of saturation in the case of single-beam transmission with source *B* alone. We have verified that this difference is not due to any thermal decay of either source *A* or *B* as we change the source configuration of the instrument.

TABLE I. Single-beam transmission and uncalibrated VCD intensities for source A, source B, and dual sources A&B and calculated A&B+A.

Source	Single-beam transmission	Uncalibrated VCD[a]
A	98	0.09
B	162	0.09
A&B	72	0.32
A&B+A	170	⋯

[a] VCD intensity measured as the intensity difference between the positive peak near 1220 cm^{-1} and the negative peak near 1130 cm^{-1}.

The values of the peak intensity of the single-beam infrared transmission curves near 1800 cm^{-1} are given in Table I for the four curves in Fig. 2. The intensity reduction factors, predicted from Eq. 17, for dual-source operation relative to source *A* and source *B*, respectively, are given by:

$$\frac{\left|a_R^s a_T^s I^A(\bar{\nu}) - a_R^p a_T^p I^B(\bar{\nu})\right|}{a_R^p a_T^p I^B(\bar{\nu})} = \frac{|98 - 162|}{162} = 0.40 \quad (18)$$

$$\frac{\left|a_R^s a_T^s I^A(\bar{\nu}) - a_R^p a_T^p I^B(\bar{\nu})\right|}{a_R^s a_T^s I^A(\bar{\nu})} = \frac{|98 - 162|}{98} = 0.65 \quad (19)$$

Comparison to the measured reduction figures of 72/162 = 0.44 and 72/98 = 0.73 confirm dual source operation as formulated theoretically.

Comparison of the uncalibrated VCD spectra (ratio of VCD transmission to IR transmission without calibration) from single-source (SS) and dual-source (DS) operation is given in Fig. 3 for the *S*-(−)-α-pinene sample in Fig. 2. From the intensity values in Table I, and using Eq. 16, one predicts an increase in the VCD intensity for DS operation relative to SS operation (for either source *A* or *B*) to be as follows:

$$[\Delta A(\bar{\nu})]_{DS} = \frac{a_R^s a_T^s I^A(\bar{\nu}) + a_R^p a_T^p I^B(\bar{\nu})}{\left|a_R^s a_T^s I^A(\bar{\nu}) - a_R^p a_T^p I^B(\bar{\nu})\right|}[\Delta A(\bar{\nu})]_{SS}$$

$$= \frac{98 + 162}{|98 - 162|}[\Delta A(\bar{\nu})]_{SS} = (4.0)[\Delta A(\bar{\nu})]_{SS} \quad (20)$$

The level of increase is verified in Fig. 3 and in Table I where the increase in size for the DS-VCD spectrum is 3.6 relative to that of each of the SS-VCD measurements.

Also displayed in Fig. 3 are the noise curves for each of these measurements. The noise at the detector is constant for each of these measurements under the expected assumption of background-noise-limited operation of the MCT detector. The VCD noise curve is not the same for each of these three measurements since the un-normalized VCD transmission, at constant noise, is divided by the single-beam IR transmission of the instrument with the sample in place in order to remove instrument-scale dependence from the VCD measurement, as in Eq. 13.

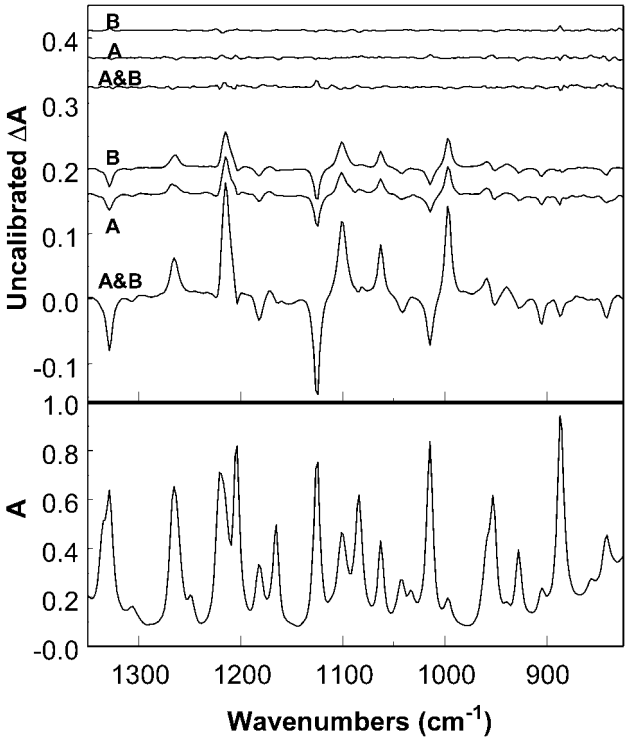

FIG. 3. (**Upper**) Uncalibrated VCD and noise spectra and (**lower**) absorbance spectra for sources **A, B,** and **A&B** for a sample of neat *S*-(−)-α-pinene in a 69 μm cell at 4 cm^{-1} resolution and a collection time of 20 min for each source configuration.

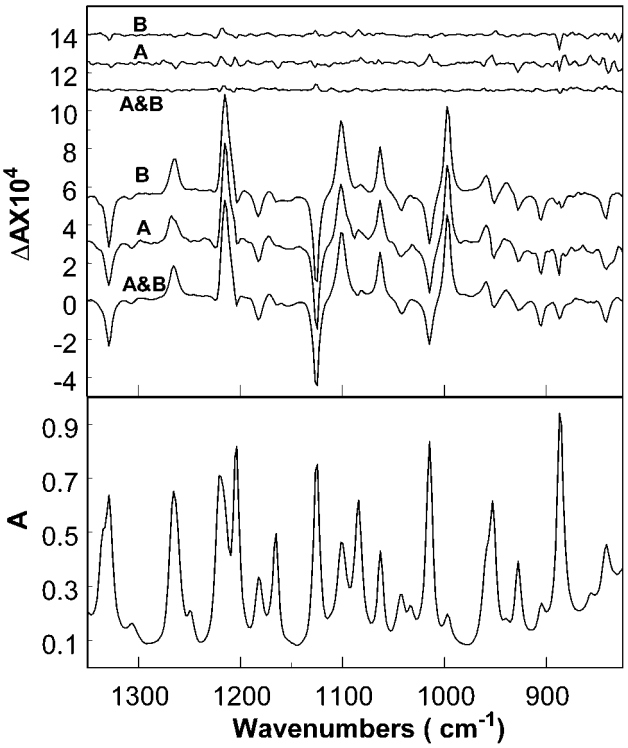

FIG. 4. (**Upper**) Calibrated VCD and noise spectra and (**lower**) absorbance for sources **A, B,** and **A&B** of *S*-(−)-α-pinene, neat in a 69 μm cell at 4 cm^{-1} and a collection time for each source configuration of 20 min.

This normalization favors higher infrared transmission intensity (smaller apparent noise due to division by a larger transmission intensity) over lower intensity, and thus the noise for operation with single-source *A* is greater than that for source *B* (the source with higher transmission), and the noise for DS operation is the largest of the three since it has the smallest transmission. However, the gain in VCD intensity for DS operation significantly outweighs the smaller increase in the VCD noise (*vide infra*).

In Fig. 4, we present absorbance and final calibrated VCD spectra with noise curves for the *S*-(−)-α-pinene for all three source settings. In this figure, all three VCD measurements, properly calibrated, yield the same VCD intensity. The only difference now is the noise level. A clear advantage is seen for DS operation, with source *B* the next best and source *A*, the weaker source, the worst result. The DS improvement in signal-to-noise ratio scales as the sum of the two source intensities over the single source intensity of reference. Relative to source *B* and source *A*, these advantages are, respectively:

$$\frac{a_R^s a_T^s I^A(\bar{\nu}) + a_R^p a_T^p I^B(\bar{\nu})}{a_R^p a_T^p I_0^B(\bar{\nu})} = \frac{98 + 162}{162} = 1.6 \quad (21)$$

$$\frac{a_R^s a_T^s I^A(\bar{\nu}) + a_R^p a_T^p I^B(\bar{\nu})}{a_R^s a_T^s I_0^A(\bar{\nu})} = \frac{98 + 162}{98} = 2.7 \quad (22)$$

The decrease in collection time for DS operation over SS operation to achieve the same signal-to-noise ratio scales is the square of these advantages, namely 2.6 relative to source *B* and 7.3 relative to source *A*.

DISCUSSION

The four-port interferometer used for these measurements is the standard optical layout for the MB-line (for example MB-100) of medium resolution FT-IR spectrometers from ABB Bomem. There are two source positions, cube-corner mirrors, and fast collection optics. The efficiencies in signal-to-noise ratio for normal single-source operation are at the state-of-the-art level and are in no way compromised by the dual-source four-port optical layout. The only optical modification needed for dual-source VCD operation is the placement of polarizers with orthogonal relative orientation before the sources. In addition to using the simultaneous dual-source operation for VCD, two sources in one instrument have been used for normal FT-IR absorption measurements with two different sources; for example, one for the mid-infrared and one for the near-infrared region have been used. The sources were not used at the same time, and one can choose which source and spectral region to study. Simultaneous dual-source operation for VCD and VLD is the subject of a recent patent application.[16]

One might be concerned that use of only the lower part of the beamsplitter for the beams coming into the beamsplitter and the upper part of the beamsplitter for the outgoing beams would decrease the efficiencies of the interferometer. However, if the source is intercepted and collimated by a mirror that is sufficiently small and close to the source, the same solid angle of light coming from the source can be captured and directed to the beamsplitter as that by a larger mirror placed further away and designed to fill the entire beamsplitter with collimated light from the source. This is the basic principle of optical

miniaturization whereby a smaller spectrometer can be designed to perform without loss of efficiency provided that all dimensions are scaled accordingly.

It is clear from Figs. 2 through 4 that the theoretical description of a four-port dual-source interferometer given above is verified with experimental measurements. In particular, we find that for ordinary infrared intensity measurements, the two sources in the common output beam, corresponding to Eq. 7, interfere with each other to reduce the magnitude of the observed interferogram. In addition, Eqs. 7 and 14 are verified for DS-VCD measurement where the magnitude of the observed uncalibrated VCD is increased relative to that for SS-VCD measurement by the ratio of additive contributions of the two sources to the subtractive contributions of the two sources, as given by Eq. 16.

The increase in the signal-to-noise ratio of the DS-VCD relative to the SS-VCD in Fig. 3 is due to the additivity of the VCD intensities coming from the two sources without an increase in the noise contribution from the detector. From the experimental results in Figs. 2 through 4, one concludes that the contribution of source *B* is greater than that for source *A* by the ratio of approximately 1.0 to 0.6. When, for VCD, the sources combine, the VCD signal increases without any increase in the accompanying noise. The signal-to-noise ratio therefore increases in this case by a factor of 1.6 compared to that of source *B* (not the normal source position for the output beam used) and a factor of 2.7 relative to source *A* (the normal source position for this output beam). This is equivalent to a decrease in spectral collection time, to achieve the same signal-to-noise ratio, of 2.6 relative to the corresponding SS-VCD measurement with source *B* and a reduction of 7.3 relative to the SS-VCD measurement with source *A*. These are very significant reductions in collection times that demonstrate a significant advantage to DS-VCD measurement compared to that of SS-VCD measurement.

A second intrinsic advantage of DS operation is the reduction of the large interferogram associated with the ordinary IR spectrum. The reduction of the magnitude of the interferogram intensity allows the normal saturation level of the detector to be avoided. In particular, for the spectra presented in Figs. 2 and 3, the intensity level of the stronger source, source *B*, without a sample in place is beyond the saturation limit of its single-source operation. Since a background intensity measurement is necessary to measure the absorbance of a sample, normally steps would need to be taken to reduce the level of this intensity. Thus, not only can we use source *B* at a level of spectral contribution that is beyond its saturation limit, but also the contribution of source *A*, the normal source position, is added to this. This gives access to an operating regime that is well beyond that of an equivalent SS-VCD spectrometer. In principle, one can envision increasing the strengths of the sources to arbitrarily large levels, such that both sources are well beyond the saturation limit, as long as the contributions of both sources are sufficiently well balanced to prevent their difference contribution from exceeding the normal SS saturation limit. There is, however, an issue that remains unexplored to date that may effectively limit the intensity levels that can be accessed by each source. This is the possible saturation of the detectors by the constant, non-Fourier-modulated intensities given by the first two terms in Eqs. 7 and 8. For the experiments performed here and to date with dual-source VCD operation, we have found no effects of detection saturation due to the non-Fourier modulated intensity at the detector.

An interesting limit of advantage of dual-source operation is when the contributions of the two sources are the same level. In this case, the DS-IR interferogram cancels and the DS-VCD doubles compared to either SS-VCD interferogram. The doubling of the VCD interferogram signal against a constant noise background leads to a doubling of the SNR and an improvement in signal averaging time of 4. Another way of stating this advantage is that the VCD spectrometer operating in DS mode under these conditions is equivalent to four such instruments operating in parallel for the same time of collection. Equal contributions from each source also maximizes the suppression of interferogram saturation since, in fact, there is no normal IR intensity spectrum. At the same time, this limit is rather inconvenient since the single-beam IR interferogram is needed to obtain the proper VCD spectrum, in accordance with Eq. 13. Hence, for exactly matched sources, some other method, such as an aperture or screen in one of the source beams, is necessary to unbalance the source intensities and obtain the single-beam IR spectrum.

Finally, we offer a few comments regarding the ease of alignment and the quality of the VCD baseline for dual-source versus single-source operation. In general, adjusting the baseline is simpler with one source compared to two. For the alignments to date where this has been carried out, the quality of the baseline achieved for two sources is the same as that obtainable with a single source. A particular concern might be the effect of moving the linear polarizer from just before the PEM in the standard single-source layout to a polarizer directly in front of each of the two sources for dual-source operation. For dual-source operation good linear polarization must be maintained over a number of mirror reflections prior to reaching the PEM. The directions of the two source polarizations are chosen to correspond to either pure *s*- or pure *p*-reflections at each mirror surface, (i.e., vertical or horizontal), and there does not appear to be any significant loss of these pure linear polarization states between the polarizers and the PEM. While the overall alignment is more difficult, there is an additional degree of freedom that can be utilized before arriving at the final alignment, namely the baseline of the second source can be used to balance that of the first source. Finally, the quality of any baseline achieved with dual-source operation can be improved by roughly one order of magnitude by using a dual-PEM setup as described in detail in an earlier publication from this laboratory.[7] The three VCD spectrometers in our laboratory at Syracuse University spanning the mid-IR to the near-IR from 800 to 10 000 cm^{-1} are all configured with two sources and two PEMs for optimum signal-to-noise ratio and baseline quality.

CONCLUSION

In this paper, we present for the first time the concept of dual-source Fourier transform polarization difference

spectroscopy. The method, which is equally applicable to circular dichroism and linear dichroism measurements, is achieved by introducing orthogonally oriented polarizers in front of two sources in a four-port interferometer. The two source locations (used one at a time) and four-port cube-corner-mirror interferometer is the standard configuration of the MB series of FT-IR and FT-NIR spectrometers available from ABB-Bomem. The design and use of a polarized dual-source, four-port interferometer for VCD operation are described theoretically and experimentally. The advantages of such an interferometer include an additive contribution of VCD (or VLD) intensities from the two sources with respect to a fixed detector noise limit (for background-limited-noise operation), and a subtractive contribution of the IR intensities from the two sources, thus avoiding saturation limits normally encountered in single-source operation.

1. L. A. Nafie, Ann. Rev. Phys. Chem. **48,** 357 (1997).
2. L. A. Nafie, in *Encyclopedia of Spectroscopy and Spectrometery*, J. C. Lindon, G. E. Tranter, and J. L. Holmes, Eds. (Academic Press, Ltd., London, 1999), p. 2391.
3. R. K. Dukor and L. A. Nafie, in *Encylopedia of Analytical Chemistry: Instrumentation and Applications*, R. A. Meyers, Ed. (John Wiley and Sons, Chichester, 2000), p. 662.
4. L. A. Nafie and T. B. Freedman, in *Circular Dichroism: Principles and Applications, Second Edition*, K. Nakanishi, N. Berova, and R. Woody, Eds. (Wiley-VCH, New York, 2000), p. 97.
5. L. A. Nafie and T. B. Freedman, in *Infrared and Raman Spectroscopy of Biological Materials*, H.-U. Gremlich and B. Yan, Eds. (Marcel Dekker, Inc., New York, 2000), p. 15.
6. L. A. Nafie, R. K. Dukor, and T. B. Freedman, in *Handbook of Vibrational Spectroscopy*, J. M. Chalmers and P. R. Griffiths, Eds. (John Wiley and Sons, Chichester, 2002), p. 731.
7. L. A. Nafie, Appl. Spectrosc. **54,** 1634 (2000).
8. L. A. Nafie and D. W. Vidrine, Proc. Soc. Photo. Inst. Eng. **191,** 56 (1979).
9. L. A. Nafie, E. D. Lipp, and C. G. Zimba, in *Proceedings of the 1981 International Conference on Fourier Transform Infrared Spectroscopy*, J. Sakal, Ed. (SPIE, Vol. 289, 1981), 457.
10. E. D. Lipp, C. G. Zimba, and L. A. Nafie, Chem. Phys. Lett. **90,** 1 (1982).
11. L. A. Nafie and M. Diem, Appl. Spectrosc. **33,** 130 (1979).
12. A. E. Dowrey and C. Marcott, Appl. Spectrosc. **36,** 414 (1982).
13. L. A. Nafie, in *Advances in Applied FTIR Spectroscopy*, M. W. Mackenzie, Ed. (John Wiley and Sons, New York, 1988), p. 67.
14. P. R. Griffiths and J. A. d. Haseth, *Fourier Transform Infrared Spectrometry* (John Wiley and Sons, New York, 1986).
15. J. Chamberlin, *Principles of Interferometric Spectrosopy* (John Wiley and Sons, New York, 1979).
16. L. A. Nafie and H. Buijs, BioTools, Inc., U.S. Patent Application (2003).